Article

Intelligent Mining of Urban Ventilated Corridor Based on Digital Surface Model under the Guidance of K-Means

Chaoxiang Chen [1,2], Shiping Ye [1,2,*], Zhican Bai [1,2], Juan Wang [1,2], Alexander Nedzved [2,3,4] and Sergey Ablameyko [2,3,4]

1   School of Information Science and Technology, Zhejiang Shuren University, Hangzhou 310015, China; ccx@zjsru.edu.cn (C.C.); 600352@zjsru.edu.cn (Z.B.); juanw@zjsru.edu.cn (J.W.)
2   International Science and Technology Cooperation Base of Zhejiang Province: Remote Sensing Image Processing and Application, Hangzhou 310000, China
3   Faculty of Applied Mathematics and Computer Science, Belarusian State University, 220004 Minsk, Belarus; nedzveda@tut.by (A.N.); ablameyko@bsu.by (S.A.)
4   United Institute of Informatics Problems of National Academy of Sciences, 220004 Minsk, Belarus
*   Correspondence: ysp@zjsru.edu.cn

Abstract: With the acceleration of urbanization, climate problems affecting human health and safe operation of cities have intensified, such as heat island effect, haze, and acid rain. Using high-resolution remote sensing mapping image data to design scientific and efficient algorithms to excavate and plan urban ventilation corridors and improve urban ventilation environment is an effective way to solve these problems. In this paper, we use unmanned aerial vehicle (UAV) tilt photography technology to obtain high-precision remote sensing image digital elevation model (DEM) and digital surface model (DSM) data, count the city's dominant wind direction in each season using long-term meteorological data, and use building height to calculate the dominant wind direction. The projection algorithm calculates the windward area density of this dominant direction. Under the guidance of K-means, the binarized windward area density map is used to determine each area and boundary of potential ventilation corridors within the threshold range, and the length and angle of each area's fitted elliptical long axis are calculated to extract the ventilation corridors that meet the criteria. On the basis of high-precision stereo remote sensing data from UAV, the paper uses image classification, segmentation, fitting, and fusion algorithms to intelligently mine potential urban ventilation corridors, and the effectiveness of the proposed method is demonstrated through a case study in Zhuji City, Zhejiang Province.

Keywords: tilt photography; DSM; urban ventilated corridor; frontal area density (FAD); K-means; intelligent mining

1. Introduction

With economic and social development, global urbanization is becoming increasingly high. According to the statistic, the urbanization worldwide was at around 56 percent in mid-2020. According to UN estimates, by 2050, over 70% of the human population will live in urban areas. Since the reform and opening-up policy, China has experienced the world's most extensive urbanization process. From 1978 to 2019, China's population of permanent urban residents increased from 172 million to 848 million, with an urbanization rate of 17.92 percent to 60.6 percent. A total of 65 percent of China's permanent population will be urbanized during the 14th Five-Year Plan period (2021–2025).

Urbanization promotes social, economic, and technological development and improves residents' employment, education, and living standards. However, when cities develop in size, buildings become higher and denser, the population increases, and more pollutants are emitted, resulting in a unique urban climate (urban heat island, urban rain island, urban cloud island, and so on). As a result, urban wind speeds decrease, calm

wind days increase, and heat island effects intensify. It also affects the urban air circulation and the diffusion of pollutants, exacerbates the formation of haze weather, causes hidden dangers of urban safety operation, and affects health [1–3].

Good ventilation promotes urban air circulation and reduces air pollution [4–6]. Building urban ventilated corridors (VC) and improving the urban ventilation environment are effective measures to improve urban air circulation capacity and alleviate the bad urban air environment [7–9].

In recent years, many scholars of urban meteorology, planning, environment, geography, and ecology have conducted a great deal of research on the mechanism, function, planning, and potential ventilation power of urban ventilated corridors. Urban ventilated corridor planning and potential ventilation power research have experienced qualitative to quantitative analysis. Xu et al. [10] analyzed the spatial distribution of urban heat islands and cool sources, based on the distribution map of the daily average temperature of typical meteorological conditions, proposed planning urban ventilation channels to alleviate urban heat islands. Su et al. [11] proposed urban ventilation corridors' location, quantity, and planning control requirements in the new urban districts. Luo et al. [12] proposed suggestions on optimization of urban ventilation from the aspects of road orientation, building layout, green space layout, and open recreation space by a case study in Lipu County of Guangxi. Wang et al. [13] took Chengdu as an example, created a spatial evaluation model of wind frequency, and planned the Urban Ventilation corridors accordingly.

In terms of quantitative calculation and simulation analysis of ventilated corridors, many scholars use CFD (computational fluid dynamics) for simulation analysis based on remote sensing and GIS data. Lu et al. [14] analyzed the influence of neighborhood distribution, building height, and square green space on urban ventilation effect by numerical simulation of CFD ventilation in the central urban area of Tonglu. Zeng [15] provided physical factors such as wind speed, wind pressure, wind speed ratio, and bad wind speed area ratio as evaluation criteria for the air ducts in Tianjin's central metropolitan area using ENVI temperature inversion and CFD software wind simulation. Wicht et al. [16] obtained 3D building database from SPOT satellite images in the year 1992, 2002 and 2011, and estimated the city's ventilation corridor by calculating roughness length and zero-plane displacement height. Yin et al. [17] proposed a complete evaluation of the ventilation effectiveness of urban built-up areas with street morphology as the center using interactive GIS and CFD numerical simulation tools. Hu et al. [18] used CFD to simulate wind environment characteristics in the winter and summer seasons, as well as in the river wind environment, in the Qiantang River region of Hangzhou, and proposed the landscape layout of different wind environment types to facilitate urban ventilation. Wang et al. [19] used three sets of digital elevation data extracted from different satellite images of Mong Kok, Hong Kong, to simulate and evaluate the ventilation environment using the LES. Yang et al. [20] conducted numerical simulations of several seasons to suggest a ventilation index based on the weighting of near-surface temperature and roughness length and developed ventilation corridors at the city size of Beijing in the winter and summer seasons.

Other scholars design their models according to urban ventilation factors to analyze ventilated corridors. For example, Wang et al. [21] established a comprehensive evaluation model for potential urban ventilated corridors by constructing the spatial dataset of five influencing factors representing the surface roughness of urban ventilated corridors (VC) in the central metropolitan area of Hangzhou to determine the maximum potential ventilated areas as potential ventilated corridor areas. Qiao et al. [22] proposed the urban ventilation network model (UVNM), which takes urban form and building height as the main factor and determines the potential ventilated corridors in Beijing through the least cost path (LCP) method. Man et al. [23] proposed the building frontal area index model and analyzed the winding path using the least cost path method. Yuan [24] took a WRF/UCM (weather research and forecasting/urban canopy model) to construct the two-stage ventilations channel under the regional scale, four city-territory-scale primary ventilations channels, and six city-territory-scale secondary ventilations channels. Peng et al. [25] proposed

"A Least Cumulative Ventilation Cost Method" to divide three-level corridors in Wuhan, which has achieved good results. Zhang [26] proposed a new model of the frontal area of coastal mountain cities to reflect the blocking effect of mountains and landforms on urban wind environment; Zeng et al. [27] identified ventilated corridors in Shanghai by using frontal area and distance between buildings. Shen et al. [28] determined the location of potential ventilated halls in Zhengzhou according to the surface roughness of underlying urban surface, with the help of ArcGIS software and LCP.

In terms of primary urban data, traditional remote sensing and GIS can only obtain brief information such as the height of buildings, which is not very accurate [29], and cannot express more detailed information such as the sides and forms of buildings. The stereo image formed by the tilting camera can observe the ground object from multiple angles and reflect the actual situation of the ground object truer. The output image may be used to perform height, length, area, tilt, and slope measurements, which greatly enhances the data's richness and accuracy and lays the foundation for future production of "true" orthographic city images and 3D city models [30].

To sum up, there are issues with studying urban ventilation corridors, such as the low resolution of traditional remote sensing image data, resulting in inaccurate parameters such as feature morphology, height, and area, and the difficulties in analyzing complex urban ventilation environments and mining potential ventilation corridors using software simulations, such as CFD [29]. In the previous studies, there has been little attention on the use of accurate data produced from UAV tilt photography to create suitable picture classification, segmentation, computation, and other relevant algorithms to quickly and reliably extract possible urban ventilation corridors.

Urban DEM and DSM are generated using tilt photography by UAV to collect high-resolution data on the city's surface, and wind direction is determined using meteorological statistics. The effect of ground roughness on urban ventilation and the density of buildings' frontal areas is studied. The frontal area density was calculated using the projection method, and the definition of urban ventilated corridors based on frontal area density was proposed. Under the guidance of K-means, the ventilation corridor is intelligently mined and extracted (extract) by FAD classification, segmentation, computation, and image algorithms such as fusion with DSM. This research takes Zhuji City, Zhejiang Province as an example, and the experimental results show the effectiveness of this research method.

2. Methodology and Data

2.1. Oblique Photography and Digital Surface Model Acquisition

2.1.1. UAV Tilt Photography

UAV is widely used for remote sensing and tilt measurement due to its convenient flight and low cost. When choosing a UAV for city tilt aerial photography, its load, endurance, and flight stability are mainly considered. The tilt aerial camera comprises a down-looking camera and several tilt cameras. A primary camera is vertically observed to obtain a vertical image, while other cameras are placed at a certain angle along the orthogonal orientation to obtain a side-view image.

Before flight shooting, UAV altitude should be determined according to the required resolution. The sailing height is computed as follows:

$$h = \frac{f * GSD}{a} \tag{1}$$

where h denotes flight height, GSD denotes ground resolution, f denotes focal length of the lens, and a denotes pixel size.

After UAV shooting, image uniformity and color uniformity processing, data inspection and correction, aerial triangulation, digital elevation model (DEM) extraction and editing, digital orthophoto map (DOM) generation and splicing, and orthophoto image quality inspection and modification are needed to make and form the required urban DEM and DSM model data.

2.1.2. Digital Elevation Model and Digital Surface Model

Much professional software supports generating DEM, DSM, and DOM from tilted photography models. The corresponding grid image data can be automatically generated by setting the map range, resolution, and camera height. DSM is the simulation of the ground surface, including the cover of vegetation and the surface of houses. DEM can be formed by processing DSM and removing information such as houses and greenery. In the early stage of the research, oblique image data were obtained by an oblique aerial camera. After digital image processing, geometric correction was made on urban map to generate DSM. The difference between DSM and DEM was used to extract the height of urban surface roughness such as buildings, rivers, lakes, and vegetation.

2.1.3. Urban Wind Environment Analysis and Ventilated Corridor Model
Determination of Urban Dominant Wind Direction

As a professional statistical chart of wind environment, a wind rose chart can quantitatively analyze the characteristics of wind direction, wind speed, and wind frequency in a particular area in a period [31].

The data of the wind rose chart come from the frequency of statistics on the wind direction in 16 directions during a time period, and the calculation formula is as follows:

$$g_n = f_n / \left(c + \sum\nolimits_n^{16} f_n\right) \qquad (2)$$

where g_n is the wind frequency in the direction n, f_n represents the number of observed winds in direction n within the statistical period, and C is the number of calm winds observed in the statistical period.

The data of the wind rose chart come from the average wind speed in all directions (except the calm wind), and the calculation formula is as follows:

$$\overline{V_n} = \sum_{i=1}^{f_n} \frac{V_{ni}}{f_n} \qquad (3)$$

$$\overline{V_c} = \sum\nolimits_{i=1}^{c} \frac{V_{ci}}{C} \qquad (4)$$

$\overline{V_n}$ represents the average wind speed in the n direction, n = 1...15, f_n represents the number of observed winds in the n direction within the statistical period; V_{ni} represents the wind speed of the ith wind observed in the n direction within the statistical period. $\overline{V_c}$ means the average wind speed of calm wind within the statistical period, C is the number of calm wind observed within the statistical period, and V_{ci} is the ith relaxed wind speed observed within the statistical period.

Urban Ventilation Environment Analysis and Frontal Area Density Calculation

The quality of urban ventilation is related to the meteorological environment, especially wind activity. The wind itself is caused by the movement of the earth and is a natural phenomenon that human beings cannot change at present. What human beings can change is the design and construction of cities, including the overall layout of city buildings, the control of building height and density, and the structure of roads, parks, water systems, green spaces, etc. Among the factors that affect the ventilation performance of various cities, frontal area density reflects the wind and ground roughness as the two most important factors. Regarding the experience of researchers at home and abroad, this research chooses this parameter as the main parameter to analyze the potential urban ventilation.

Frontal area density (FAD) represents the ratio between the frontal area of a building and the parcel area of the building under a specific wind direction at a certain height of increment [8]. The calculation formula of frontal area density is as follows:

$$\lambda_{f(z,\theta)} = \frac{A(\theta)_{proj(z)}}{A_T} \tag{5}$$

$A(\theta)_{proj(z)}$ is the frontal area of a building perpendicular to a specific wind direction; A_T is the parcel area (the size of the grid) where the building is located; θ is a selected wind direction; Z is height increment (the calculation range of the height of the building).

Frontal area density $\lambda_{f(z,\theta)}$ is related to wind direction. Depending on the wind direction, the corresponding building section perpendicular to the wind direction is different, and the value of $\lambda_{f(z,\theta)}$ is also different. Frontal area density reflects the obstructing effect of urban form on wind in a specific order; that is, it demonstrates the ventilation capacity of current in a particular direction in a metropolitan area.

According to the above definition of frontal area density, it is necessary to classify the height of urban buildings and determine the height increment. In this research, DSM and DEM generated by UAV oblique photography are used, and Global Mapping and other software are used to perform the difference diagram corresponding to DSM and corresponding DEM. The ground roughness image is generated to extract the high data of urban buildings and calculate height increment.

The urban winter and summer wind charts' high-frequency wind direction was selected, respectively. The dominant wind direction angle (0 degrees due north) was obtained through analysis and statistics. The urban ground roughness image was rotated to be perpendicular to the wind direction angle. To calculate FAD, a series of grid data files were generated according to the specified grid scale, such as 50 m × 50 m and 100 m × 100 m. These data files contain spatial distribution and height data information for all buildings.

In this research, the height increment image projection method is used to calculate the windward area of buildings in each grid, and then divided by the grid area to automatically calculate the frontal area density of each grid. During the projection, the ground objects low to the ground (such as small shrubs) and ground objects of small width (such as telephone poles) should be filtered by defining the threshold. Figure 1 shows the calculation process of frontal density area.

Definition of Urban Ventilated Corridors

With the frontal area density as the main factor, the length of ventilated corridor refers to the continuous size of the interval value of the frontal area density.

Figure 2 shows the inverse relationship between FAD and the parabolic wind speed ratio. The smaller the FAD value, the smaller the obstruction through the area, and the higher the wind speed, the better the ventilation efficiency.

Based on the empirical data, the quantitative description is as follows:

- FAD ≤ 0.35 indicates that the natural wind enters smoothly;
- 0.35 < FAD ≤ 0.45 indicates that the natural wind is not smooth enough;
- 0.45 < FAD ≤ 0.65 indicated that natural wind was obstructed;
- FAD > 0.65 indicates a significant obstacle to natural wind entry.

Combined with the specifications of climatic feasibility demonstration to design urban ventilated corridors to meet the People's Republic of China Meteorological Industry Standard, drawing on the research experience of domestic and foreign scholars, in this research, the following three empirical data are selected as the minimum standards of ventilated corridors in small and medium-sized cities:

(1) FAD < 0.35;
(2) VC length > 1000 m;
(3) VC width ≮ 50 m;
(4) θ (angle between VC strike and dominant wind direction) < 45°.
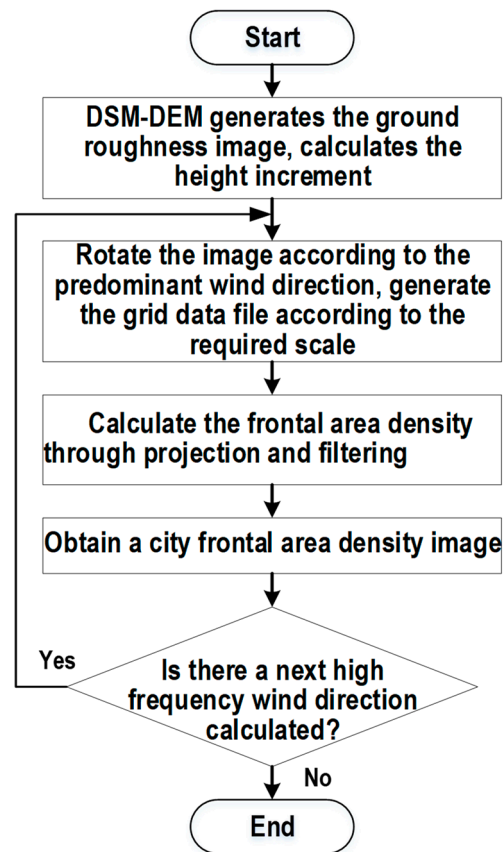
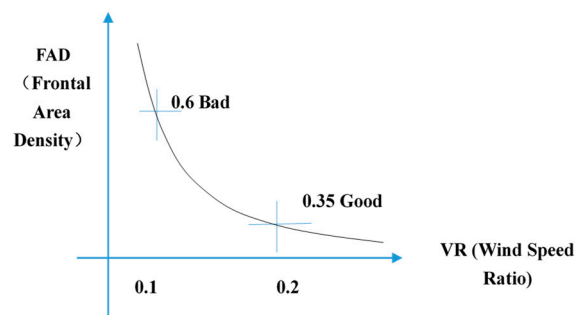**Figure 1.** Calculation flow of frontal area density of urban buildings.

Figure 2. Relationship between frontal area density and wind speed ratio.

In urban planning, ventilated corridors are related to the size of the city. To describe the urban ventilation potential in more detail, this research classifies the ventilation corridors of small and medium-sized towns into three levels: CCI, CCII, and CCIII. Parameters are as follows (Table 1):

Table 1. Wind scales of ventilation corridors in small and medium-sized planned cities.

	CCI	CCII	CCIII
VC length (m)	Well versed	$\geq$2000	(1000, 2000)
VC width (m)	$\geq$200	(80, 200)	(50, 80)
θ	<30°	<45°	<45°

2.2. Ventilated Corridor Mining Method Based on K-means

2.2.1. K-Means Algorithm

K-means is a standard clustering algorithm in unsupervised learning, widely used in various classifications.

The K-means model uses a k-means clustering algorithm that divides a set of data into several distinct categories to test this hypothesis. This means that the distance between the data in each variety should be very close; in other words, the closer the data are, the more similar the data should be. The processing procedure of the k-means algorithm is as follows: Firstly, k samples are randomly selected, and each model initially represents the mean value or center of a cluster; for each remaining model, it is assigned to the nearest set according to its distance to each cluster center. The average value of each group is then recalculated. This process is repeated until the criterion function converges.

The algorithm steps are as follows:

(a) Select the initial k category centers μ_1, μ_2 ⋯ ⋯ , μ_{k-1}, μ_k

(b) For each sample, mark it as the category closest to the center of the category, i.e.,

$$label_i = \underset{1 \leq j \leq k}{\operatorname{argmin}} \, ||x_i - \mu_j|| \tag{6}$$

(c) Update the center of each category to the mean value of all samples belonging to the category.

$$\mu_j = \frac{1}{|C_j|} \sum_{i \in c_j} x_j \tag{7}$$

(d) Repeat the last two steps until the change in the category center is less than a certain threshold.

2.2.2. Interactive Mining of Urban Ventilated Corridors

On the basis of obtaining the urban FAD diagram, k-means calculation and a small amount of interaction are carried out to generate ventilated corridors according to the above classification experience values of ventilated corridors in small and medium-sized cities. These operations are performed to generate eligible ventilation corridors at all levels through the calculation and condition judgment of the fitted ellipse long axis and angle of the potential ventilation corridor area of the binary image. Figure 3 shows the process.

2.2.3. Generation and Discrimination of Urban Ventilated Corridors

After clustering the FAD at each level, the image is binarized, i.e., pixels with FAD < 0.35 are set to 1 and pixels with FAD $\geq$ 0.35 are set to 0, to form a binary map of multiple regions containing potential ventilation corridors. At the same time, using the clustered image and the actual DSM image, the 0 and 1 values of individual pixels are manually reset to show the areas that could be excellent for ventilation.

To extract the borders of these regions, the binary map is traversed and each region with a value of 1 is recorded. There are many methods for extracting boundaries, such as the Canny operator, the Prewitt operator, and the Sobel operator. We use the simplest processing method because this study only deals with binary image regions. In particular, we set the left side of the region from left to right "0, 1, 1" to "0, 1, 0", the upper part of the region from top to bottom "0, 1, 1" to "0, 1, 0", the right side of the region from right to left "1, 1, 0" to "0, 1, 0", the lower part of the region from top to bottom "1, 1, 0" to "0, 1, 0", and all other pixel values are set to 0.

After the regional boundary is extracted, the ellipse is fitted by obtaining the coordinates of multiple points, including the extreme values, and the long axis and angle of the ellipse are calculated to discern whether the length is in accordance with the length of the

ventilation corridor at all levels and the angle with the dominant wind direction, as shown in Figure 4.
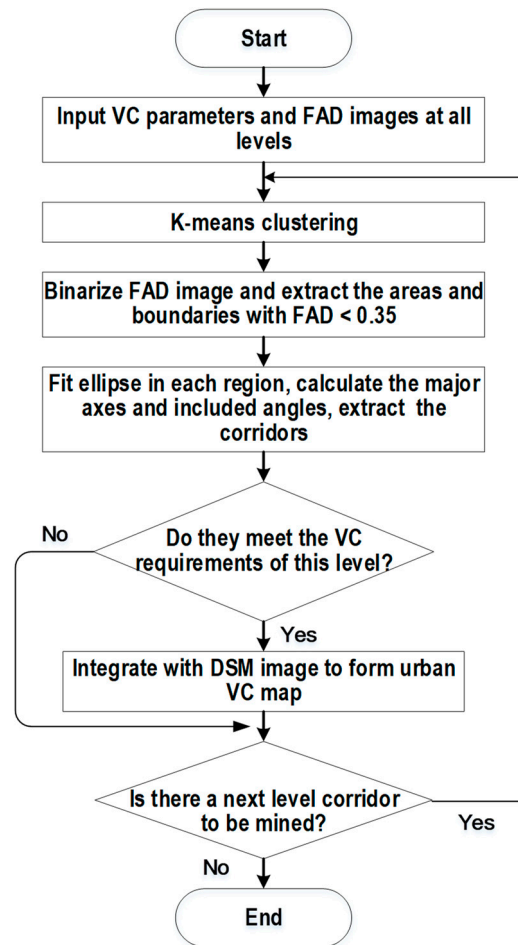

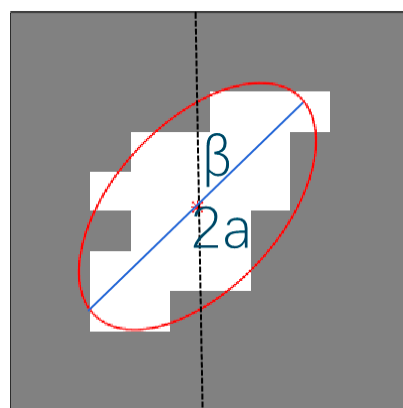**Figure 3.** Flow chart of ventilated corridor mining.

Figure 4. Computation of the length and angle of the long axis by fitting an ellipse.

We designed the method as follows. Denote the selected n data as $(x_i, y_i)(i = 1, 2, \ldots, n)$, and assume that the fitted elliptic equation is

$$x^2 + Bxy + Cy^2 + Dx + Ey - 1 = 0 \tag{8}$$

Then, we have

$$Ax_i^2 + Bx_iy_i + Cy_i^2 + Dx_i + Ey_i - 1 = \varepsilon_i \tag{9}$$

where ε_i is the perturbation error, then the total deviation.

$$Q = \sum_{i=1}^{n} \varepsilon_i^2 = \sum_{i=1}^{n} \left(Ax_i^2 + Bx_iy_i + Cy_i^2 + Dx_i + Ey_i - 1 \right)^2 \tag{10}$$

To minimize Q, the following should be satisfied:

$$\frac{\partial Q}{\partial A} = 0, \frac{\partial Q}{\partial B} = 0, \frac{\partial Q}{\partial C} = 0, \frac{\partial Q}{\partial D} = 0, \frac{\partial Q}{\partial E} = 0,$$

i.e.,

$$
\begin{cases}
\frac{\partial Q}{\partial A} = 4 \sum_{i=1}^{n} \varepsilon_i x_i^2 = 4 \sum_{i=1}^{n} \left(Ax_i^4 + Bx_i^3 y_i + Cx_i^2 y_i^2 + Dx_i^3 + Ex_i^2 y_i - x_i^2 \right) = 0 \\
\frac{\partial Q}{\partial B} = 2 \sum_{i=1}^{n} \varepsilon_i x_i y_i = 2 \sum_{i=1}^{n} \left(Ax_i^3 y_i + Bx_i^2 y_i^2 + Cx_i y_i^3 + Dx_i^2 y_i + Ex_i y_i^2 - x_i y_i \right) = 0 \\
\frac{\partial Q}{\partial C} = 4 \sum_{i=1}^{n} \varepsilon_i y_i^2 = 4 \sum_{i=1}^{n} \left(Ax_i^2 y_i^2 + Bx_i y_i^3 + Cy_i^4 + Dx_i y_i^2 + Ey_i^3 - y_i^2 \right) = 0 \\
\frac{\partial Q}{\partial D} = 2 \sum_{i=1}^{n} \varepsilon_i x_i = 2 \sum_{i=1}^{n} \left(Ax_i^3 + Bx_i^2 y_i + Cx_i y_i^2 + Dx_i^2 + Ex_i y_i - x_i \right) = 0 \\
\frac{\partial Q}{\partial E} = 2 \sum_{i=1}^{n} \varepsilon_i y_i = 2 \sum_{i=1}^{n} \left(Ax_i^2 y_i + Bx_i y_i^2 + Cy_i^3 + Dx_i y_i + Ey_i^2 - y_i \right) = 0
\end{cases}
$$

For simplicity, we denote $\overline{x^K y^L} = \frac{1}{n}$, (K,L = 0,1,2,3,4).
The matrix form of the above equation is

$$
\begin{pmatrix}
\overline{x^4} & \overline{x^3 y} & \overline{x^2 y^2} & \overline{x^3} & \overline{x^2 y} \\
\overline{x^3 y} & \overline{x^2 y^2} & \overline{xy^3} & \overline{xy^3} & \overline{xy^2} \\
\overline{x^2 y^2} & \overline{xy^2} & \overline{y^4} & \overline{xy^2} & \overline{y^3} \\
\overline{x^3} & \overline{x^2 y} & \overline{xy^2} & \overline{x^2} & \overline{xy} \\
\overline{x^2 y} & \overline{xy^2} & \overline{x^3} & \overline{xy} & \overline{y^2}
\end{pmatrix}
\begin{pmatrix}
A \\ B \\ C \\ D \\ E
\end{pmatrix}
=
\begin{pmatrix}
\overline{x^2} \\ \overline{xy} \\ \overline{y^2} \\ \overline{x} \\ \overline{y}
\end{pmatrix}
$$

The following can be verified:

$$
R\left(
\begin{pmatrix}
\overline{x^4} & \overline{x^3 y} & \overline{x^2 y^2} & \overline{x^3} & \overline{x^2 y} & \overline{x^2} \\
\overline{x^3 y} & \overline{x^2 y^2} & \overline{xy^3} & \overline{xy^3} & \overline{xy^2} & \overline{xy} \\
\overline{x^2 y^2} & \overline{xy^2} & \overline{y^4} & \overline{xy^2} & \overline{y^3} & \overline{y^2} \\
\overline{x^3} & \overline{x^2 y} & \overline{xy^2} & \overline{x^2} & \overline{xy} & \overline{x} \\
\overline{x^2 y} & \overline{xy^2} & \overline{x^3} & \overline{xy} & \overline{y^2} & \overline{y}
\end{pmatrix}
\right)
= R\left(
\begin{pmatrix}
\overline{x^4} & \overline{x^3 y} & \overline{x^2 y^2} & \overline{x^3} & \overline{x^2 y} \\
\overline{x^3 y} & \overline{x^2 y^2} & \overline{xy^3} & \overline{xy^3} & \overline{xy^2} \\
\overline{x^2 y^2} & \overline{xy^2} & \overline{y^4} & \overline{xy^2} & \overline{y^3} \\
\overline{x^3} & \overline{x^2 y} & \overline{xy^2} & \overline{x^2} & \overline{xy} \\
\overline{x^2 y} & \overline{xy^2} & \overline{x^3} & \overline{xy} & \overline{y^2}
\end{pmatrix}
\right)
$$

The unique solution (A,B,C,D,E) of the above equation can be determined, and Equation (8) can be obtained, whose geometric center (h,k) as follows:

$$
\begin{cases}
h = \dfrac{\begin{vmatrix} -D & B \\ -E & 2C \end{vmatrix}}{\begin{vmatrix} 2A & B \\ B & 2C \end{vmatrix}} \\[20pt]
k = \dfrac{\begin{vmatrix} 2A & -D \\ B & -E \end{vmatrix}}{\begin{vmatrix} 2A & B \\ B & 2C \end{vmatrix}}
\end{cases}
$$

When $B > 0$:

$$\text{Elliptic long axis } 2a = 2\sqrt{\frac{2 - Dh - Ek}{A + C - \sqrt{(A - C)^2 + B^2}}}$$

$$\text{Elliptic short axis } 2b = 2\sqrt{\frac{2 - Dh - Ek}{A + C + \sqrt{(A - C)^2 + B^2}}}$$

The rotation angle (angle with the *y*-axis) $\beta = \frac{1}{2}arccot\frac{A-C}{B}$, $(0 \leq 2\beta < \pi)$.
When $B < 0$:

$$\text{Elliptic long axis } 2a = 2\sqrt{\frac{2 - Dh - Ek}{A + C + \sqrt{(A - C)^2 + B^2}}}$$

$$\text{Elliptic short axis } 2b = 2\sqrt{\frac{2 - Dh - Ek}{A + C - \sqrt{(A - C)^2 + B^2}}}$$

The rotation angle (angle with the *y*-axis) $\beta = 90 - \frac{1}{2}arccot\frac{A-C}{B}$, $(0 \leq 2\beta < \pi)$.

We can discriminate whether the corridor is a ventilation corridor as follows: 2a*grid length ≥ the corridor length at that level, | *β-dominant wind direction* | ≤ the angle standard at that level (30 degrees for CCI, 45 degrees for CCII and CCIII), and also the extracted corridor width pixel*grid length ≥ the corridor width at that level.

2.3. Data

2.3.1. Calculation of Data and Related Parameters in the Study Area

This research takes the Zhuji City of Zhejiang Province as the research object. Zhuji is located in the northeast of central Zhejiang Province and the southwest of Shaoxing, which is a subtropical monsoon climate zone with four distinct seasons, more rainfall, sufficient light, an annual average temperature of 16.3 °C, and a perennial average precipitation of about 1373.6 mm. It covers an area of more than 2310 square kilometers and has a population of more than 1.2 million. The urban area is more than 60 square kilometers and the population is more than 300,000

We used UAV tilt photography and post-processing to gather DEM, DSM, and DOM images of the urban area, and obtained nearly two decades of meteorological data from the city's meteorological department.

Roughness and Dominant Wind Direction in Zhuji Urban Area

According to the subtraction operation of DSM and DEM, the height of each point of roughness in the urban area is obtained. The surface roughness image of the Zhuji urban area is shown in Figure 5.

Figure 5. Surface roughness image of the Zhuji urban area.

The urban buildings were counted after removing street trees and telegraph poles, as shown in Figure 6. Buildings with height of 25 m or less accounted for 96.83% of the total, so the height increment of urban areas is 25 m.
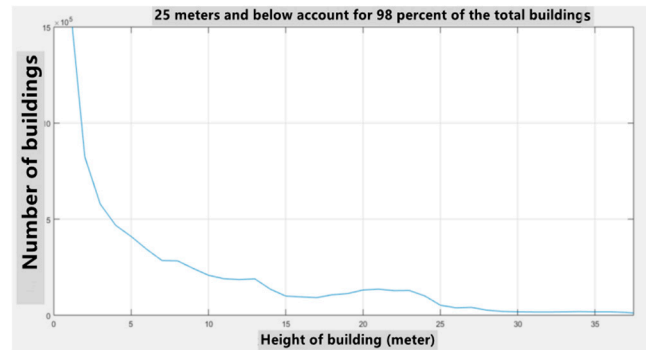

Figure 6. Building height distribution in the Zhuji urban area.

We obtained the data of daily average wind speed and wind direction at the height of 10 m in the city for the recent 20 years from the meteorological department of this city, and made the following wind rose charts shown in Figure 7a,b.

(**a**)   (**b**)
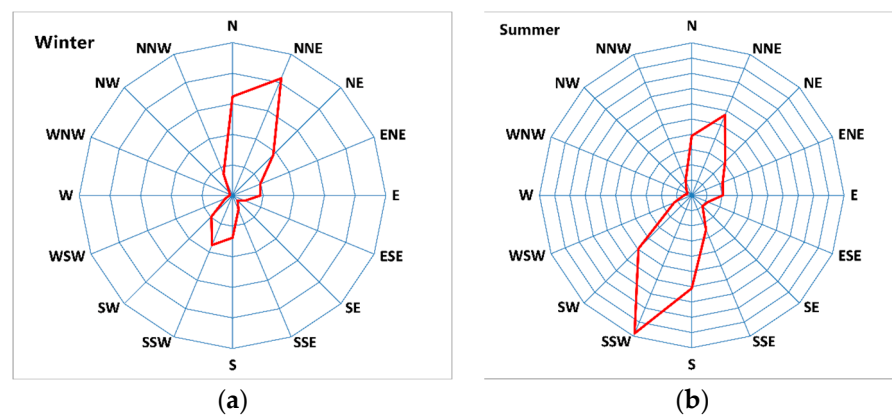
Figure 7. Urban wind rose chart in the Zhuji urban area. (**a**) Wind rose chart in winter; (**b**)wind rose chart in summer.

Figure 6 shows that the dominant wind direction in winter in Zhuji is obvious: NNE (north–northeast) and N (north). The frequencies of these two wind directions are 20.75% and 16.2%, respectively, and the sum of the frequencies is 36.95%. The weighted average wind direction angle is NE 12.64 degrees.

The dominant wind direction in Zhuji in summer is SSW (south–southwest) and S (south). The frequencies of these two wind directions are 19.6% and 12.2%, respectively, and the sum of frequencies is 31.8%. The weighted average wind direction angle is 193.87 degrees, SW 13.87 degrees.

FAD in Zhuji Urban Area

According to the dominant wind direction, the frontal area density of the Zhuji urban area in winter and summer is calculated by dividing it into 50 m grids, as shown in Figure 8 below.
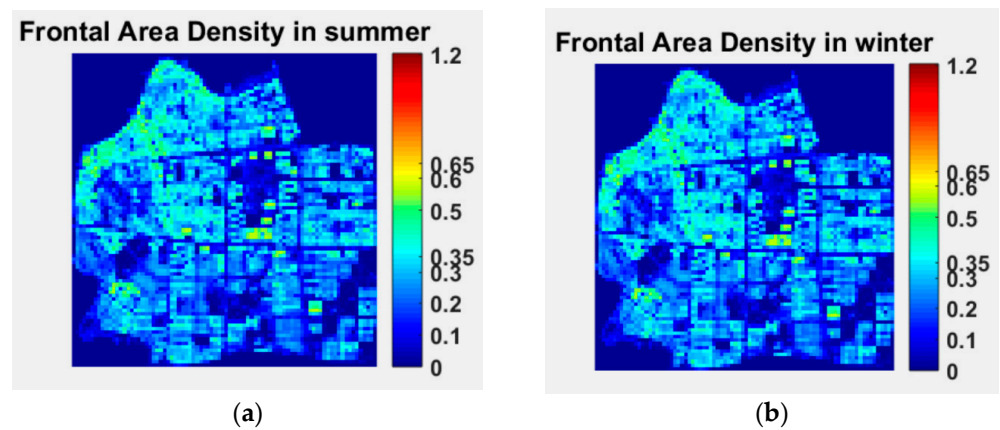
Figure 8. Frontal area density map in the Zhuji urban area. (**a**) FAD in summer; (**b**) FAD in winter.

3. Result

3.1. Ventilated Corridor Mining Experiment

3.1.1. Experimental Environment

Server: Lenovo ThinkSystem SR650, GPU: NVIDIA Tesla V100 32 GB, MEMORY: 256 GB DDR4 2666 MHz, CPU: 2 PCS Inter(R) Xeon(R) Gold 5117 CPU @ 2.00 GHz, OS: 64 Windows Server 2016. Other software systems are MATLABR2019, Global Mapper 17. In this research, the "Urban Ventilated Corridor Mining System" is developed to provide users with intelligent ventilation corridor mining with only a few interface interactions.

3.1.2. Mining Process of Ventilated Corridor

In this research, for FAD clustering of the frontal area density of the case city, assuming k = 1–5, the clustering range and median value are obtained to have a general impression of the case city FAD distribution. Based on the empirical importance of various literature, the FAD value of the ventilated corridor area should be less than 0.35. Based on this, according to the general classification of ventilation potential into excellent, good, acceptable and poor, set K = 4, using K-means clustering, obtains <0.04, 0.14~0.25, and 0.25~0.34 for four categories, which are represented, respectively, by progressive color changes from blue to red, as shown in Figure 9.
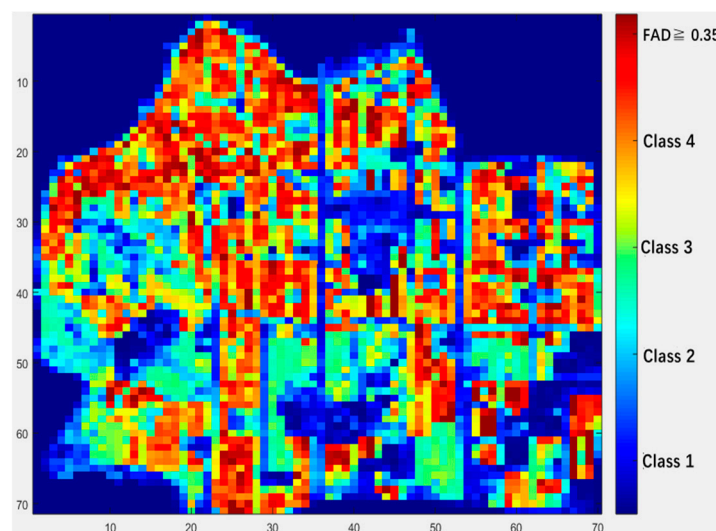

Figure 9. After clustering when FAD < 0.35 and K = 4.

This graph is converted into a binary chart with FAD < 0.35 in the system to ease mining. Corridor parameters are input on the interactive interface, such as width ≥ 80 m,

length $\geq$ 2000 m, and angle < 450 with the dominant wind direction. The system automatically extracts each area with pixel value of 1 for FAD < 0.35 to form a binary map with potential ventilation corridors. See Figure 10.
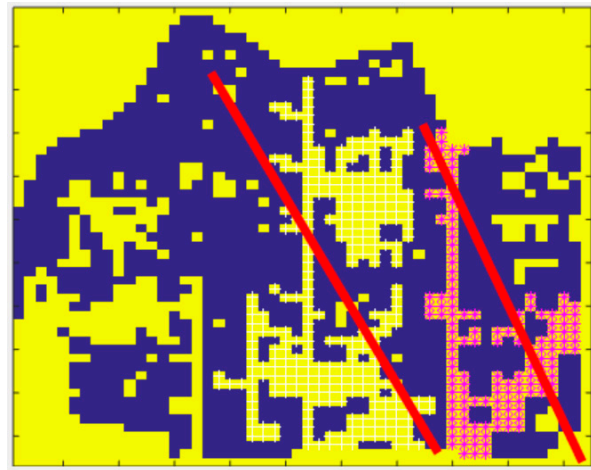

Figure 10. Automatically forming a large area that meets the requirements. (The red lines are the diagonal of 2 large rectangular area).

The system is automatically associated with the urban DSM map. The operator can segment a large area by connecting or disconnecting individual FAD points (resetting these points) according to the actual situation to form a place close to the width of the ventilated corridor, as shown in Figure 11.
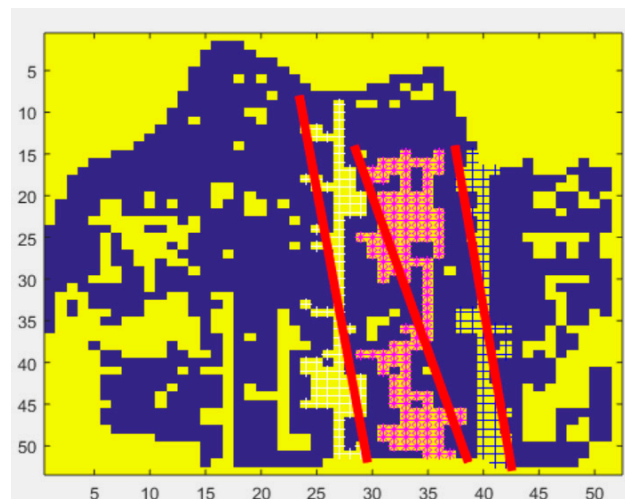

Figure 11. Dividing and forming several smaller areas conforming to the ventilated corridor conditions. (The red lines are the diagonal of the 3 smaller rectangular areas.)

Simultaneously, the system determines whether the long axis of the ellipse to be synthesized in each region meets the length of the corridor at that level, whether the angle between the long axis' direction and the dominant wind direction of the season (e.g., NE 22.5 degrees in winter) is less than the angle of the corridor level, and whether the corridor width meets the requirements of the corridor at that level. After deleting all unsatisfied regions, the system can extract the satisfied corridors. See Figure 12.
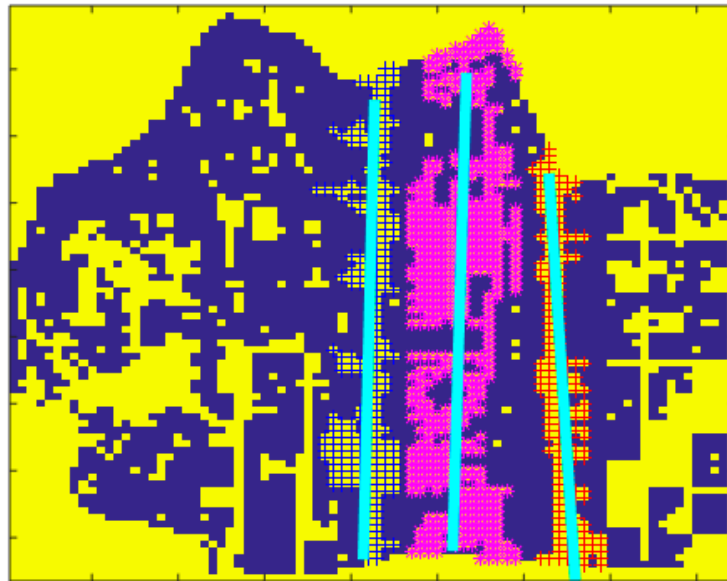
Figure 12. Extraction of the ventilation corridor that meets the conditions of this level. (The blue lines are the prototypes of three general ventilation corridors.)

Finally, the system overlays the mined ventilated corridor area that meets the original urban DSM map conditions. The accurate ventilated corridor is formed by B spline algorithm, as shown in Figure 13.

Figure 13. Ventilated corridor is fitted by the B-spline algorithm.

3.2. Mining Results of Ventilated Corridor

In this research, the first-, second-, and third-level corridor mining is carried out in Zhuji city. The dominant wind direction in winter is selected. The minimum width is 200 m, which runs through the town, and the angle between corridor direction and the prevailing wind direction is <30 degrees as the standard, and the result shows that there is no first-level corridor in this area.

The dominant wind direction in winter was selected. The minimum width was 80 m, the minimum length was 2000 m, the angle between corridor direction and the prevailing wind direction was <45 degrees as the standard, and the system mined three corridors,

which can provide a reference for the secondary ventilated corridor in the urban ventilation system (Figure 14). The mining results show that no. 1 and no. 3 corridors introduce natural wind into urban areas from the outskirts, and the spatial carrier is the urban main trunk roads. The no. 2 corridor starts from the citizen park and forms a continuous channel along the low and sparse plots of buildings such as squares, middle schools and kindergartens.
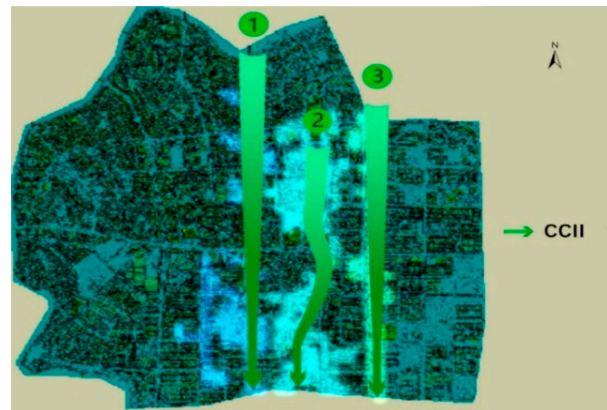

Figure 14. Automatic mining results of 80-m-wide and 2000-m-long secondary corridor.

With the minimum width of 50 m and a minimum length of 1000 m, and the angle between corridor direction and dominant wind direction <45 degrees as the standard, the system mined five ventilated corridors, which can be used as the third-level reference of urban ventilation system (Figure 15). The no. 1 corridor originates from a large city square and forms a continuous corridor along with green land and enterprise land. The space carrier of the no. 2 and no. 3 corridor is the urban road. The no. 4 corridor starts from the countryside, passing primary schools, low-intensity residential, and other land; the no. 5 corridor relies on space carrier for undeveloped urban land, enterprise land, and so on. The detailed data of the mined results are shown in Table 2.
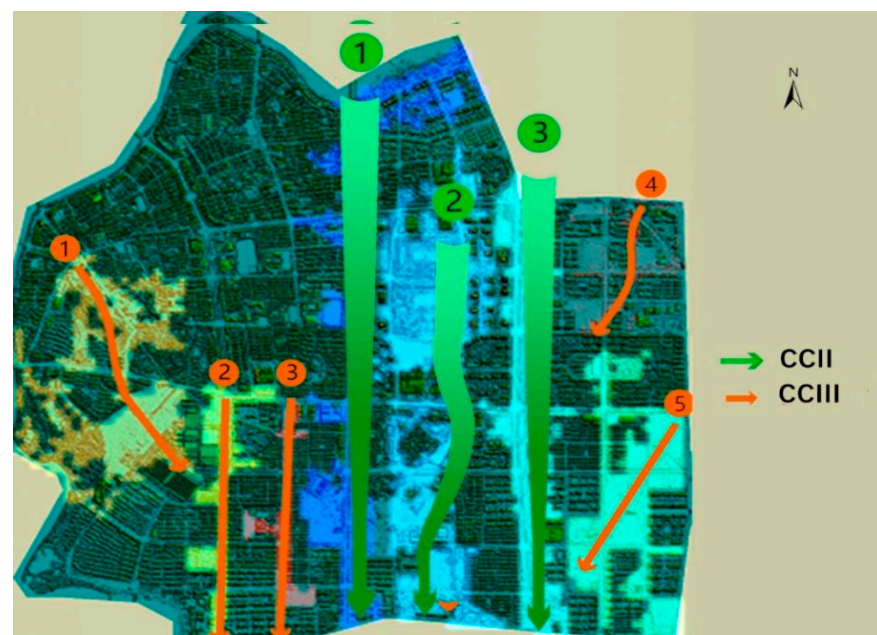

Figure 15. Results of corridor excavation in Zhuji City.

Table 2. Data of ventilation corridor in Zhuji City.

	CCII-1	CCII-2	CCII-3	CCIII-1	CCIII-2	CCIII-3	CCIII-4	CCIII-5
Length (m)	4212	4192	3701	1810	1805	2002	1088	1819
Direction (°)	NE 4.15	NE 0.78	NW 2.8	NW 20	NE 2.6	NW 1.1	NW 21.7	NW 5.1
Width (m)	(80,200)	(80,200)	(80,200)	(50,80)	(50,80)	(50,80)	(50,80)	(50,80)

In this research, three teachers from the Planning and Design major of the School of Urban Construction of Zhejiang Shuren University were invited to manually draw the ventilated corridor roughly according to the first-, second-, and third-level conditions without knowing the system mining results. The average overlap rate of the results was >95%, as shown in Table 3. The validity of this research method is illustrated.

Table 3. Comparison of system mining and expert recommendation results.

	Number of First-Level Corridors	Number of Second-Level Corridors	Number of Third-Level Corridors	Corridor Location Consistency	Corridor Length Consistency
System	0	3	5	100%	100%
Expert 1	0	3	5	94.3%	95.7%
Expert 2	0	3	5	95.2%	94.8%
Expert 3	0	3	5	95.4%	96.5%

4. Discussion

From the perspective of data, we use the remote sensing data in this study. Rapid urbanization and industrialization have resulted in a slew of air pollution issues in cities, necessitating the exploration of prospective ventilation corridors in order to alter urban structure and control urban climate. Because of their vast coverage and short acquisition intervals, high-resolution remote sensing images have become a significant database for analyzing cities. Compared to optical remote sensing satellites for obtaining urban data, which are often affected by clouds, shadows, and other factors, as well as drawbacks such as the difficulty of obtaining feature elevation data, UAV tilt photography for obtaining high-precision stereo data has significant advantages and is expected to become the primary method for obtaining urban data in the future.

From the perspective of methods, we design an efficient K-means-based method for mining urban ventilation corridors. Windward area density is the most important indicator of urban ventilation (FAD). This study calculates the urban windward area density (FAD) of dominant wind direction by projecting building height in each grid using the difference between DSM and DEM created by high-precision stereo data obtained from UAV tilt photography; the obtained FAD data of each network is accurate, and the calculation method is efficient and simple. The length and angle of the fitted elliptical long axis of each area are calculated to extract ventilation corridors that meet the criteria, and the binarized windward area density map is guided by K-means to extract each area and boundary of potential ventilation corridors within the threshold range. In the instance city of Zhuji City, Zhejiang Province, the method was experimentally evaluated, and the excavation results were more accurate.

From the perspective of implication, we believe this work can contribute to the advancement of urban environmental research and management. Traditional urban ventilation corridor planning is created by urban and rural planning experts using their professional knowledge, and the planning and design outcomes are based on the city's objective construction environment while also taking into account the designers' subjective design consciousness. Urban ventilation corridor planning is, to some part, the outcome of a subjective–objective interaction, and the scientificity of planning necessitates the use

of exact data, correct methodologies, scientific theories, and systematic design. The algorithm utilized in this study for gathering urban data and extracting urban ventilation corridor mining provides technical support for more scientific urban ventilation corridor development. With the rapid pace of global urbanization, a growing number of cities are confronted with issues such as environmental degradation and urban heat waves. The larger the city, the more apparent the dilemma becomes, and the planning and construction of urban ventilation corridors becomes increasingly important. The database and technique design have been validated to be applicable to big and medium-sized cities and can be extended to cities of various scales to aid urban and rural planners in design and government decision-making.

However, there are still some limitations of this study. Except for a small number of interactive time-linked DSM maps with reference to actual situational and physical scenes, this study primarily depends on the FAD index to examine urban ventilation corridors, and other influencing factors are not planned to be explored in a complete index. Furthermore, the results are not well-presented to local officials.

In the future, we plan to continue the research in two areas: (1) make full use of tilt remote sensing data to investigate the impact of various factors of urban roughness on the city's potential ventilation capacity, in order to more comprehensively and accurately excavate the city's ventilation corridors and provide virtual reality technical support for accurate microclimate environment planning and design; and (2) investigate computer simulation technology to show how the city's potential ventilation capacity is affected by various factors of urban roughness.

5. Conclusions

To improve the urban ventilation environment and protect the health of people living in the city, it is necessary to excavate and design ventilation corridors to solve the problems of heat island effect and air pollution generated by urbanization. The following are the study's main findings: (1) Remote sensing data obtained by UAV tilt photography has high resolution, accurate data on the morphology and height of buildings, easy access, and low cost, making it a useful database for analyzing the current state of cities, planning urban layout, and governing the urban environment. (2) Calculating the urban windward area density (FAD) of dominating wind direction by the direction of building height projection using the difference between DSM and DEM is a realistic and efficient method. (3) The algorithm for excavating the ventilation corridor described in this paper is efficient and accurate. It binarizes the FAD map in the empirical threshold range with K-means guidance, extracts each area and boundary that meet the threshold conditions, fits the ellipse and calculates the long axis length, angle, and other parameters, and extracts the ventilation corridors that meet the conditions by comparing and discriminating with the set ventilation corridor conditions at each level.

In the future, we aim to investigate the impact of various urban roughness characteristics on the city's potential ventilation capacity to more thoroughly and precisely explore the city's ventilation corridors and to provide technological assistance for accurate microclimate environment planning and design.

Institutional Review Board Statement: Not applicable.

Informed Consent Statement: Not applicable.

Data Availability Statement: Not applicable.

Conflicts of Interest: The authors declare no conflict of interest.

References

1.   Fang, X.-Y.; Li, L.; Liu, W.; Ren, C.; Wang, J.-W.; Cheng, C.; Yu, Y.; Zhang, S.; Du, W.-P.; Liu, Y.-H. Progress of researches and practices of urban ventilation corridor in China. *Chin. J. Ecol.* **2021**, *40*, 4088–4098. [CrossRef]
2.   Gu, K.K.; Fang, Y.H.; Qian, Z.; Sun, Z.; Wang, A. Spatial planning for urban ventilation corridors by urban climatology. *Ecosyst. Health Sustain.* **2020**, *6*, 1747946. [CrossRef]
3.   Tian, L.; Li, Y.; Lu, J.; Wang, J. Review on Urban Heat Island in China: Methods, Its Impact on Buildings Energy Demand and Mitigation Strategies. *Sustainability* **2021**, *13*, 762. [CrossRef]
4.   Ren, C.; Yang, R.; Cheng, C.; Xing, P.; Fang, X.; Zhang, S.; Wang, H.; Shi, Y.; Zhang, X.; Kwok, Y.T.; et al. Creating breathing cities by adopting urban ventilation assessment and wind corridor plan—The implementation in Chinese cities. *J. Wind. Eng. Ind. Aerodyn.* **2018**, *182*, 170–188. [CrossRef]
5.   Lenzholzer, S.; Carsjens, G.-J.; Brown, R.D.; Tavares, S.; Vanos, J.; Kim, Y.; Lee, K. Urban climate awareness and urgency to adapt: An international overview. *Urban Clim.* **2020**, *33*, 100667. [CrossRef]
6.   Kress, R. *Regionale Luftaustausc Hprozesse und Ihre Bedeutung fur die Raumliche Planung*; Institut for Umweltschutz der Universitat Dortmund: Dortmund, Germany, 1979.
7.   Xu, Y.; Wang, W.; Chen, B.; Chang, M.; Wang, X. Identification of ventilation corridors using backward trajectory simulations in Beijing. *Sustain. Cities Soc.* **2021**, *70*, 102889. [CrossRef]
8.   Zhu, Y.L.; Yu, L.L.; Ding, S.G. The application of urban ventilation channel for urban environment improvement. *Urban Stud.* **2008**, *15*, 46–49.
9.   Hsieh, C.M.; Huang, H.C. Mitigating urban heat islands: A method to identify potential wind corridor for cooling and ventilation. *Comput. Environ. Urban Syst.* **2016**, *57*, 130–143. [CrossRef]
10.   Xu, D.; Zhou, D. Research on the Planning Methods of Mitigating Summer Urban Heat Island Effects among Basin Cities—A Case Study at Xi'an, China. *Procedia Eng.* **2016**, *169*, 248–255. [CrossRef]
11.   Su, N.; Zhou, D.; Jiang, X. Study on the Application of Ventilation Corridor Planning in Urban New Area-A Case Study of Xixian New Area. *Procedia Eng.* **2016**, *169*, 340–349. [CrossRef]
12.   Luo, Y.; He, J.; Ni, Y. Analysis of urban ventilation potential using rule-based modeling. Comput. Environ. *Urban Syst.* **2017**, *66*, 13–22. [CrossRef]
13.   Wang, X.; Gao, F.; Tan, Q.; Xiao, Z. Planning for Ventilation Corridor in City with High-Frequency Static Wind: A Case Study of Chengdu City. *City Plan. Rev.* **2020**, *44*, 129–136. [CrossRef]
14.   Lu, L.; Li, D.; Wang, Z.Y.; Wang, J.-K.; Yang, Z. Study on the numerical simulation and optimization setting for the city ventilation corridors. *Zhejiang Constr.* **2015**, *32*, 49–54. [CrossRef]
15.   Zeng, H. *Research on the Theory of "Source-Flow-Sink" Ventilated Corridor System Construction and Planning Strategy—The Case of the Center Districts of Tianjin*; Tianjin University: Tianjin, China, 2016.
16.   Wicht, M.; Wicht, A.; Osinskaskotak, K. Detection of ventilation corridors using a spatio-temporal approach aided by remote sensing data. *Eur. J. Remote Sens.* **2017**, *50*, 254–267. [CrossRef]
17.   Yin, J.; Zhan, Q. Urban Street Wind Path Research Based on GIS and CFD—A Case Study of Wuhan. *Chin. Landsc. Archit.* **2019**, *35*, 84–88. [CrossRef]
18.   Hu, J.; Xie, J.; Wang, Y. Simulation of Wind Environment and Exploration of Landscape Design Strategy in Qiantang River Block of Hangzhou Based on CFD Digital Technology. *Gard. Gard.* **2020**, *17*, 122–123. [CrossRef]
19.   Wang, W.; Xu, Y.; Ng, E.Y.Y.; Raasch, S. Evaluation of satellite-derived building height extraction by CFD simulations: Acase study of neighborhood-scale ventilation in Hong Kong. *Landsc. Urban Plan.* **2018**, *170*, 90–102. [CrossRef]
20.   Yang, T.S.; Wang, W.W.; Chang, M.; Wang, X. Numerical simulation and comprehensive identification of potential wind corridors in Beijing. *J. Geo-Inf. Sci.* **2020**, *22*, 1996–2009. [CrossRef]
21.   Wang, W.-W.; Li, F.-N.; Wang, D.; Wang, Q. Urban ventilation corridor construction based on ventilation potential and quantitative analysis of wind characteristics. *J. Zhejiang Univ. (Eng. Sci.)* **2019**, *53*, 69–80. [CrossRef]
22.   Qiao, Z.; Xu, X.; Wu, F.; Luo, W.; Wang, F.; Liu, L.; Sun, Z. Urban ventilation network model: A case study of the core zone of capital function in Beijing metropolitan area. *J. Clean. Prod.* **2017**, *168*, 526–535. [CrossRef]
23.   Man, S.W.; Niched, J.E.; To, P.H.; Wang, J. A Simple Method for Designation of Urban Ventilation Corridors and Its Application to Urban Heat Island Analysis. *Build. Environ.* **2010**, *45*, 1880–1889.

24. Yuan, Z. *The Research of Multi-Scale Urban Ventilation Channel Construction Method and Planning Strategy: A Case Study of Xian*; Xibei University: Shanxi, China, 2017.

25. Xie, P.; Liu, D.; Liu, Y.; Liu, Y. A Least Cumulative Ventilation Cost Method for Urban Ventilation Environment Analysis. *Complexity* **2020**, *2020*, 9015923. [CrossRef]

26. Zhang, H. Ventilation Paths Excavation and Design Strategy of Coastal Mountainous City Based on Frontal Area. Ph.D. Thesis, Dalian University of Technology, Dalian, China, 2020.

27. Zeng, S.; Qin, Y.; Chen, Y. Analysis of the Identification and Impact of Urban Ventilation Corridors in Shanghai. *J. Donghua Univ. (Nat. Sci.)* **2018**, *44*, 107–111.

28. Shen, X.J.; Zhao, R.; He, R.Z.; Wang, Q.; Guo, Y. Research on Urban Wind Environment Simulation: A Case Study of Zhengzhou Central Area. *J. Geo-Inf. Sci.* **2020**, *22*, 1349–1357. [CrossRef]

29. Ai, J. Application of Aerial Photogrammetry Technology in Fanjiagedi Topographic Survey Project. *Huabei Nat. Resour.* **2020**, *5*, 99–101.

30. Li, Y.; Su, G.; Lin, Z. Study on the Method of Extracting High Precision DEM from Oblique Image. *Bull. Surv. Mapp.* **2017**, *2*, 30–34. [CrossRef]

31. Bing, D.; Zhaoyin, Y.; Wupeng, D.; Xiaoyi, F.; Yonghong, L.; Chen, C.; Yan, L. Cooling the city with "natural wind": Construction strategy of Urban Ventilation Corridors in China. *IOP Conf. Ser. Earth Environ. Sci.* **2021**, *657*, 012009. [CrossRef]